

# Dalton Transactions

Accepted Manuscript



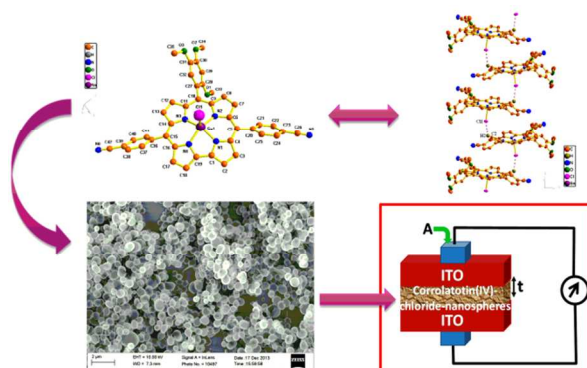
This is an *Accepted Manuscript*, which has been through the Royal Society of Chemistry peer review process and has been accepted for publication.

*Accepted Manuscripts* are published online shortly after acceptance, before technical editing, formatting and proof reading. Using this free service, authors can make their results available to the community, in citable form, before we publish the edited article. We will replace this *Accepted Manuscript* with the edited and formatted *Advance Article* as soon as it is available.

You can find more information about *Accepted Manuscripts* in the [Information for Authors](#).

Please note that technical editing may introduce minor changes to the text and/or graphics, which may alter content. The journal's standard [Terms & Conditions](#) and the [Ethical guidelines](#) still apply. In no event shall the Royal Society of Chemistry be held responsible for any errors or omissions in this *Accepted Manuscript* or any consequences arising from the use of any information it contains.

## Graphical abstract



A device was fabricated with the help of tin(IV)corrole nanospheres and its conduction properties have been measured.

Cite this: DOI: 10.1039/c0xx00000x

www.rsc.org/xxxxxx

ARTICLE TYPE

## Semi-insulating behaviour of self-assembled tin(IV)corrole nanospheres

Woormileela Sinha,<sup>a</sup> Mohit Kumar,<sup>b</sup> Antara Garai,<sup>a</sup> Chandra Shekhar Purohit,<sup>a</sup> Tapobrata Som<sup>\*b</sup> and Sanjib Kar<sup>\*a</sup>

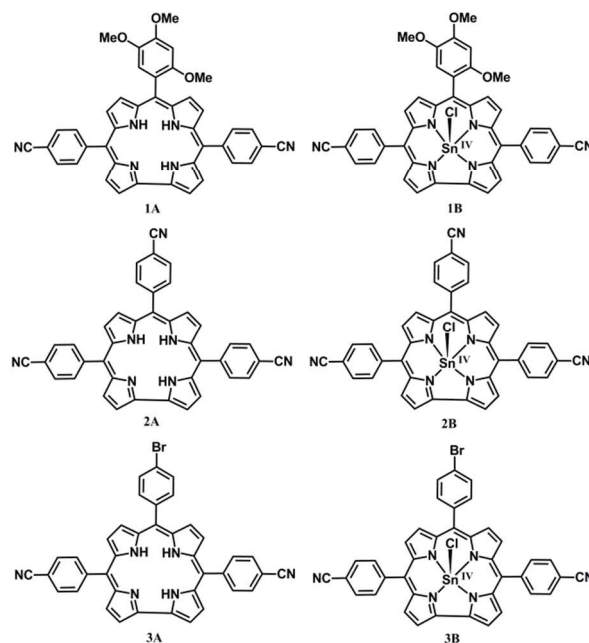
Received (in XXX, XXX) Xth XXXXXXXXX 20XX, Accepted Xth XXXXXXXXX 20XX

DOI: 10.1039/b000000x

Three novel tin(IV)corrole complexes have been prepared and characterized by various spectroscopic techniques including single crystal X-Ray structural analysis. Packing diagrams of the tin(IV)corroles revealed that corrolato-tin(IV)-chloride molecules are interconnected by intermolecular C–H...Cl hydrogen bonding interaction. H...Cl distances are 2.848 Å, 3.051 Å, and 2.915 Å respectively for the complexes. In addition, C–H...Cl angles are 119.72°, 144.70°, and 147.08° respectively for the complexes. It was also observed that in one of the three synthesized complexes, dimers are formed while in the other two cases 1D infinite polymer chains are formed. Well-defined and nicely organized three-dimensional hollow nanospheres (SEM images on silicon wafers) with diameters of ca. 676 nm and 661 nm are obtained in the complexes forming 1D polymer chains. By applying thin layer of tin(IV)corrole nanospheres, on ITO surface (AFM height images of ITO films; ~200 nm in height), a device was fabricated with the following compositions: Ag/ITO-coated glass/tin(IV)corrole nanospheres/ITO-coated glass/Ag. On calculating the resistivity ( $\rho$ ) of the nanostructured film, it was found to be  $\sim 2.4 \times 10^8 \Omega \cdot \text{cm}$ , which falls in the range of semi-insulating semiconductor. CAFM current maps at 10 V bias show bright spots with 10–20 pA intensity and indicate that the nano-spheres (~250 nm in diameter) are the electron-conducting pathways in the device. The semi-insulating behavior arises due to the non-facile electron transfer in HOMOs of the tin(IV)corrole nanospheres.

## Introduction

Green plants use chlorophyll (magnesium porphyrin) aggregates for light harvesting purposes in the nature.<sup>1, 2</sup> Inspired by this natural phenomenon, a large number of researchers are actively involved to mimic the light harvesting complexes found in green plants and purple bacteria.<sup>3-11</sup> The ultimate aim of studying the model systems of light-harvesting complexes is to gain a deeper insight into the aggregated porphyrin/metalloporphyrin structures and their unique functions mediated by the excitonic interactions between the adjacent magnesium porphyrin units in the highly ordered aggregates, and to decipher the knowledge for the construction of newer and efficient classes of bio-inspired devices. Thus the generation of porphyrin/metalloporphyrin nanostructures (e.g., nano sphere, nano tubes, etc.) and their efficient uses for various device fabrications are of utmost importance for the development of modern electronic devices.<sup>12-15</sup> In present work, a series of novel Sn(IV) corrole complexes has been synthesized (Scheme 1). The identity of the tin complexes has been established by various spectral techniques. The crystal structures of 10-(2,4,5-trimethoxyphenyl)-5,15-bis(4-cyanophenyl)corrolato-tin(IV)-chloride, **1B**, 5,10,15-tris(4-cyanophenyl)corrolato-tin(IV) chloride, **2B** and 10-(4-bromophenyl)-5,15-bis(4-cyanophenyl)corrolato-tin(IV)-chloride, **3B** are also reported here. Introduction of a series of electron releasing (like -OMe) and -withdrawing (like -CN) groups in the



**Scheme 1** Structures of the A<sub>3</sub>-corrole **2A**, and *trans*-A<sub>2</sub>B-corroles **1A** and **3A** and the corresponding corrolato-tin(IV)-chlorides, 10-(2,4,5-trimethoxyphenyl)-5,15-bis(4-cyanophenyl)corrolato-tin(IV)-chloride, **1B**, 5,10,15-tris(4-cyanophenyl)corrolato-tin(IV)-chloride, **2B** and 10-(4-bromophenyl)-5,15-bis(4-cyanophenyl)corrolato-tin(IV)-chloride, **3B**.

corrole frameworks will not only influence the energies of the molecular orbitals of the respective metal complexes but also will make them as useful precursors for the construction of various other metallo-corrole based supramolecular architectures.

Corrole,<sup>16</sup> a contracted porphyrin analogue, is recently gaining a lot of interest in research because of their potential superiority in terms of photophysical properties compared to their analogous porphyrin derivatives.<sup>17-45</sup> Among the various metallo-porphyrins, research in the field of tin complexes has also gained impetus in the recent years. These tin complexes may find suitable use for designing of various optoelectronic based materials. Although expected to be a more potent candidate than analogous Sn(IV) porphyrin complexes,<sup>46</sup> surprisingly Sn(IV) corrole based systems are rarely reported in the literature.<sup>47</sup> Self assembled supramolecular Sn(IV) corrole frameworks, in the form of nanospheres have been synthesized by using noncovalent intermolecular hydrogen bonding interactions in case of **1B** and **3B** and then one of them has been explored in the field of device fabrication. Although a sizeable number of literature reports cover the generation of Sn(IV) porphyrin based aggregates and their various applications,<sup>48</sup> however, no reports are yet available that describe the synthesis and application of Sn(IV) corrole based aggregates.

Thus the outline of the present work revolves around the synthesis, structural and spectral characterization of three novel tin(IV)corrole complexes, generation of their aggregates in the form of nanospheres and application of those nanospheres in the fabrication of semi-insulating semiconductor device. Semi-insulating semiconductors have found extensive applications in high speed microelectronic devices, isolation between devices, and also as sensing materials, like radiation sensor.<sup>49</sup> These semi-insulators are also frequently used in high-electron-mobility transistors (HEMT) which serve as the back bone of today's cell phone devices.<sup>50</sup>

## Results and discussion

### Synthesis and Characterization

The free base corroles<sup>51</sup> were prepared according to the general procedure of corrole synthesis.<sup>52</sup> For an example, 2,4,5-trimethoxy benzaldehyde and 5-(4-Cyanophenyl)dipyrromethane were dissolved in methanol and subsequent oxidation by *p*-chloranil resulted in the formation of corrole, **1A**.<sup>51</sup> The corrolato-tin(IV)-chlorides were synthesized by following a reported synthetic protocol.<sup>47</sup> In a standard protocol a mixture of corrole and the tin chloride were refluxed in a solution of DMF and resulted in the formation of corrolato-tin(IV)-chlorides in good yields. Purity and identity of the corrolato-tin(IV)-chlorides, **1B**, **2B**, and **3B** are demonstrated by their satisfactory elemental analyses and by the electro-spray mass spectra (see Experimental Section).

### UV-Vis and Emission spectra

All the three Sn(IV) corroles **1B**, **2B**, and **3B** exhibited  $\pi \rightarrow \pi^*$  transitions in the ranges 400-650 nm (Fig. S1†). All the three Sn(IV) corroles exhibit strong fluorescence in the red-regions of the visible spectra at room temperature in dichloromethane solvent (Fig. 1).<sup>41</sup>

### NMR spectra

The <sup>1</sup>H NMR spectrum of **1B** exhibits peaks in accordance with eighteen partially overlapping aromatic protons in the region,  $\delta = 9.28-6.94$  ppm (Fig. S4†). Four multiplets at  $\delta = 9.28-9.25$ , 9.09-9.03, 8.87-8.85, and 8.81-8.79 ppm are easily distinguishable and are assigned as  $\beta$ - pyrrolic hydrogen atoms. The aryl ring protons are observed at 8.12-6.94 ppm region. Out of these signals two singlets are easily distinguishable at 7.78, and 6.94 ppm. These singlets are assigned as aromatic hydrogen from 2,4,5-trimethoxyphenyl group. The three methoxy group protons are observed at 4.19, 4.01, and 3.37 ppm. The <sup>1</sup>H NMR spectrum of **2B** also exhibits peaks for twenty partially overlapping aromatic protons in the region,  $\delta = 9.36-7.84$  ppm (Fig. S5†). The <sup>1</sup>H NMR spectrum of **3B** exhibits peaks corresponding to twenty partially overlapping aromatic protons in the region,  $\delta = 9.33-7.82$  ppm (Fig. S6†). All the signals in the corrolato-tin(IV)-chlorides derivatives show downfield shift compared to free base corroles. The <sup>1</sup>H NMR data thus unequivocally establish the diamagnetic nature of the tin complexes **1B-3B**.

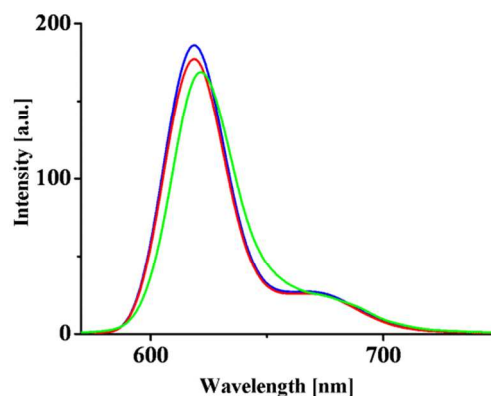


Fig. 1 Electronic emission spectrum of **1B**, (green line), **2B**, (red line) and **3B**, (blue line) (Color online) in dichloromethane ( $\lambda_{\text{ex}} = 423$  nm).

### Structures

The crystal structures of **1B**, **2B**, and **3B** are shown in Fig. S7†, Fig. S8†, and Fig. S9† respectively. The crystal systems are monoclinic, triclinic, and triclinic and the unit cells have four, two, and two corrolato-tin(IV)-chloride molecules for **1B**, **2B**, and **3B** respectively. Important crystallographic parameters for all the three complexes are presented in Table 1. Bond distances and angles are comparable with the previously reported other corrolato-tin(IV) molecules.<sup>47</sup> Tin atoms in all the three complexes **1B**, **2B** and **3B** are penta-coordinated and the geometry around the tin atom is distorted square-pyramidal in all the studied complexes. Vertical displacement of the peripheral carbon atoms from the N4 corrole planes signifies the distortion level in all the three corrole complexes (Fig. S10†).<sup>53</sup> Tin atom does not perfectly fit inside the corrole cavity of none of the three complexes; instead it is deviated from the N4 corrole planes by

**Table 1** Crystallographic Data for 10-(2,4,5-trimethoxyphenyl)-5,15-bis(4-cyanophenyl)corrolato-tin(IV)-chloride, **1B**, 5,10,15-tris(4-cyanophenyl)corrolato-tin(IV)-chloride, **2B** and 10-(4-bromophenyl)-5,15-bis(4-cyanophenyl)corrolato-tin(IV)-chloride, **3B**.

compound codes	<b>1B</b>	<b>2B</b>	<b>3B</b>
molecular formula	C <sub>42</sub> H <sub>27</sub> ClN <sub>6</sub> O <sub>3</sub> Sn	C <sub>40</sub> H <sub>20</sub> ClN <sub>7</sub> Sn	C <sub>39</sub> H <sub>20</sub> BrClN <sub>6</sub> Sn
Fw	817.84	752.77	806.66
Radiation	MoK $\alpha$	MoK $\alpha$	MoK $\alpha$
crystal symmetry	Monoclinic	Triclinic	Triclinic
space group	P21/c	P-1	P-1
<i>a</i> (Å)	17.9986(12)	12.020(5)	8.258(5)
<i>b</i> (Å)	12.5973(9)	13.221(5)	15.261(5)
<i>c</i> (Å)	16.2495(10)	15.690(5)	16.642(5)
$\alpha$ (deg)	90	93.566(5)	111.107(5)
$\beta$ (deg)	97.845(3)	109.752(5)	103.712(5)
$\gamma$ (deg)	90	106.513(5)	98.450(5)
<i>V</i> (Å <sup>3</sup> )	3649.8(4)	2215.0(14)	1837.3(14)
Z	4	2	2
$\mu$ (mm <sup>-1</sup> )	0.822	0.668	1.890
<i>T</i> (K)	293(2)	293(2)	293(2) K
<i>D</i> <sub>calcd</sub> (g cm <sup>-3</sup> )	1.488	1.129	1.458
2 $\theta$ range (deg)	4.52 to 60.3	3.45 to 29.63	1.48 to 30.55
<i>e</i> data ( <i>R</i> <sub>int</sub> )	10701 (0.0897)	12221 (0.0384)	11113 (0.0275)
R1 ( <i>I</i> > 2 $\sigma$ ( <i>I</i> ))	0.0513	0.0456	0.0403
WR2 (all data)	0.1435	0.1243	0.1287
GOF	1.041	1.096	1.009
Largest diff. peak and hole(e <sup>-</sup> Å <sup>-3</sup> )	1.112 and -0.785	1.471 and -1.909	2.415 and -1.680

5 distances of 0.6130(3) Å, 0.6516(4) Å and 0.6290(4) Å in **1B**, **2B**  
 and **3B** respectively giving rise to domed conformations in all the  
 three cases. This leads to a consequent deviation of the pyrrole  
 ring nitrogen atoms from the 19-atom corrole carbon ring by  
 distances ranging from 0.0233–0.3601 Å in **1B**. The *meso*-  
 10 substituted phenyl rings are tilted with respect to the 19-atom  
 corrole carbon plane by dihedral angles ranging from  
 48.728–65.135°. In the packing diagram of the corrolato-tin(IV)-  
 chloride molecules (**1B**), cyanide groups of two adjacent  
 corrolato-tin(IV)-chloride molecules are facing towards the same  
 15 direction, however methoxy groups of two adjacent corroles are  
 facing in the opposite direction. The distance between two  
 neighboring Sn(IV) atoms is 8.12 Å. Careful observation of the  
 packing diagram of **1B** reveals that it is actually an assembly of  
 one dimensional (1D) polymeric chains composed of corrolato-  
 tin(IV)-chloride molecules interconnected by intermolecular C-  
 H...Cl hydrogen bonding interaction (Fig. 2). The C-H...Cl  
 20 hydrogen bonding interaction<sup>54</sup> [Bonding parameters of C-  
 H...Cl; H...Cl: 2.848Å; C...Cl: 3.405 Å;  $\angle$ C-H...Cl: 119.72°]  
 is the driving force for this kind of supramolecular 1D chain  
 25 formation and this interaction is rather genuine in nature as is  
 shown by its bonding parameters in the bracket. However these

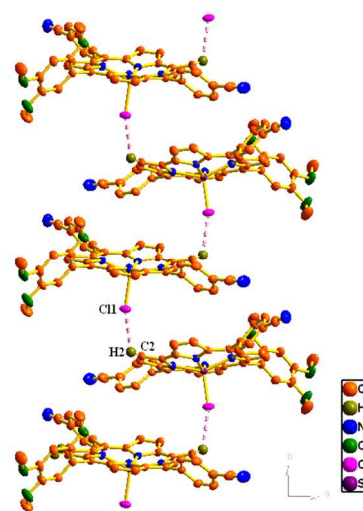


**Fig. 2** Single-crystal X-ray structure analysis of **1B**; C2-H2...Cl1 hydrogen bonding interaction [Bonding parameters of C-H...Cl {*D*<sup>i</sup> - H<sup>i</sup> ... A: C2-H2...Cl1; H... A: 2.848 Å; *D*...A: 3.405 Å;  $\angle$ D-H...A: 119.72°, symmetry codes: (i) 1 - x, -0.5 + y, 0.5 - z}].

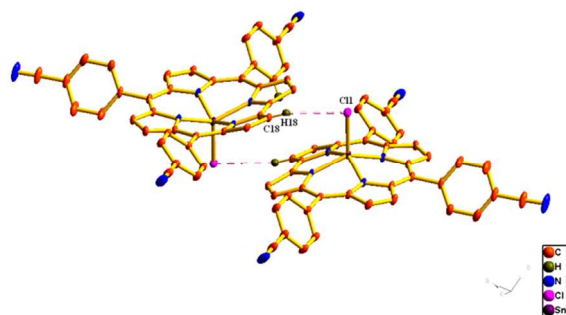


**Fig. 3** Single-crystal X-ray structure analysis of **2B**; C18–H18...Cl1 { $D^j - H^i \cdots A$ } hydrogen bonding interaction [Bonding parameters of C18–H18...Cl1; H18...Cl1: 3.051 Å; C18...Cl1: 3.849 Å;  $\angle$ C18–H18...Cl1: 144.70°, symmetry codes: (i) 1–x, 1–y, 1–z].

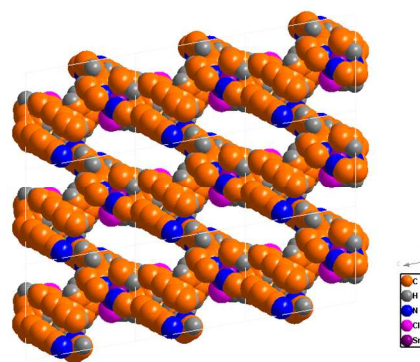


**Fig. 4** Space filling representation of the rectangular channels (dimension = 16 × 7 Å) in the crystal structure of 5,10,15-tris(4-cyanophenyl)corrolato-tin(IV)-chloride, **2B**.

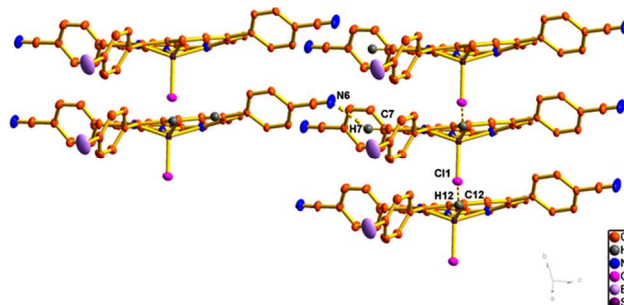


**Fig. 5** Single-crystal X-ray structure analysis of **3B**; C12–H12...Cl1 { $D-H \cdots A$ } hydrogen bonding interaction [Bonding parameters of C12–H12...Cl1; H12...Cl1: 2.915 Å; C12...Cl1: 3.730 Å;  $\angle$ C12–H12...Cl1: 147.08°, symmetry codes: (i) –1+ x, y, z], and C7–H7...N6 { $D^j - H^i \cdots A$ } hydrogen bonding interactions [Bonding parameters of C7–H7...N6; H7...N6: 2.595 Å; C7...N6: 3.285 Å;  $\angle$ C7–H7...N6: 131.32°, symmetry codes: (i) 2–x, 1–y, –z].

one-dimensional (1D) polymeric chains in **1B** are not interconnected instead they are independent of each other.  $\pi$ – $\pi$  stacking interactions (the shortest distance between two carbon atoms of the interacting rings was 3.98 Å) exist between the C36–C37–C38–C39–C40–C41 (phenyl ring) and C20–C21–C22–C23–C24–C25 (phenyl ring) in the packing diagram. C–H... $\pi$  interactions also exist in the structure, e.g. between C24–H24 and C36–C37–C38–C39–C40–C41 (phenyl ring), C37–H37 and N2–C6–C7–C8–C9 (pyrrole ring). Due to the distorted square-pyramidal geometry around the central metal atom, the pyrrole ring nitrogen atoms deviate from the 19-atom corrole carbon ring by distances of 0.1239–0.4317 Å in case of **2B** also. The *meso*-substituted phenyl rings make dihedral angles ranging from 47.204–65.049° with the corrole plane. Analysis of the packing diagram of **2B** reveals that two neighbouring corrolato-tin(IV)-chloride molecules are interconnected by intermolecular C–H...Cl hydrogen bonding interactions and form dimer (Fig. 3). The C–H...Cl hydrogen bonding interaction [Bonding parameters of C18–H18...Cl1; H18...Cl1: 3.051 Å; C18...Cl1: 3.849 Å;  $\angle$ C18–H18...Cl1: 144.70°] dictates such kind of dimer formation. The distance between two Sn(IV) ion in the dimer is 6.985 Å. However these dimers are not interconnected instead they are arranged independently in a particular fashion throughout the crystal lattice. Along the crystallographic *b*-axis, they form rectangular channel (dimension = 16 × 7 Å) like arrangements (Fig. 4).  $\pi$ – $\pi$  stacking interactions (the shortest distance between two carbon atoms of the interacting rings was 3.38 Å) exist between the C34–C35–C36–C37–C38–C39 (phenyl ring) and the all four pyrrole rings of corrole in the packing diagram. In addition to that,  $\pi$ – $\pi$  stacking interactions also exist between the N3–C11–C12–C13–C14 (pyrrole ring) and N4–C16–C17–C18–C19 (pyrrole ring). Pyrrole ring nitrogen atoms undergo deviation by distances ranging from (–0.3179) – (+0.0619) Å with respect to the corrole plane in **3B**. Dihedral angles between the *meso*-substituted phenyl rings and the corrole plane range from 48.727–61.52°. In the packing diagram of the corrolato-tin(IV)-chloride molecules (**3B**), cyanide and bromide groups of two adjacent corrolato-tin(IV)-chloride molecules are facing towards the same direction. The distance between two neighbouring Sn(IV) ion is 8.258(5) Å. Packing diagram of **3B** indicates that it

is actually an assembly of one dimensional (1D) linear polymeric chains composed of corrolato-tin(IV)-chloride molecules, interconnected by intermolecular C–H...Cl hydrogen bonding interaction. This kind of supramolecular 1D linear chain formation is mainly aided by the C–H...Cl hydrogen bonding interactions [Bonding parameters of C–H...Cl; H...Cl: 2.915 Å; C...Cl: 3.730 Å;  $\angle$ C–H...Cl: 147.08°] (Fig. 5). Two of these linear 1D polymeric chains in **3B** are interconnected by C–H...N hydrogen bonding interactions [Bonding parameters of C–H...N; H...N: 2.595 Å; C...N: 3.285 Å;  $\angle$ C–H...N: 131.32°] and forms a duplex structure. Thus the tin corroles, as described herein, can assemble on intermolecular level through C–H...Cl hydrogen bonding interactions. H...Cl distances are 2.848 Å, 3.051 Å, and 2.915 Å for **1B**, **2B**, and **3B** respectively. In addition,  $\angle$ C–H...Cl angles are 119.72°, 144.70°, and 147.08° for **1B**, **2B**, and **3B** respectively. Although these distances are very close to the van der Waals cut-off distance (3.0 Å) for H...Cl hydrogen bonding, however, a plenty of literature reports suggest that these interactions should be considered as genuine C–H...Cl hydrogen bonding interactions.<sup>54</sup> Fine tuning of these intermolecular hydrogen bonding interactions leads to different kind of architectures; linear chains, and molecular sieves. For three of the above mentioned 1D supramolecular networks, it was observed that in one case it forms dimers and in other two cases it forms 1D infinite polymer chains.

### Self aggregates of tin(IV)corroles

The nano-aggregates of tin corroles were developed in dichloromethane (DCM) and petroleum ether solvent mixture and after drop casting was dried in open air, on a silicon wafer. The generated aggregates were then examined by using SEM and AFM techniques. The SEM images of the aggregates are shown in Fig. 6 and Fig. 8 respectively. In the cases of complexes **1B** and **3B**, well defined and nicely organized three-dimensional hollow nanospheres with diameter of ca. 676 nm (Fig. 6 and Fig. 7) and 661 nm (Fig. 8 and Fig. 9) were obtained. However in the case of complex **2B**, no such three-dimensional well organized objects were obtained. These observations can be explained with the help of Srinivasarao model.<sup>55</sup> According to this model, any molecular material, when dissolved in a solvent or solvent mixture denser than water and dried in open air, gives rise to two-dimensional air bubbles for those molecules where negligible

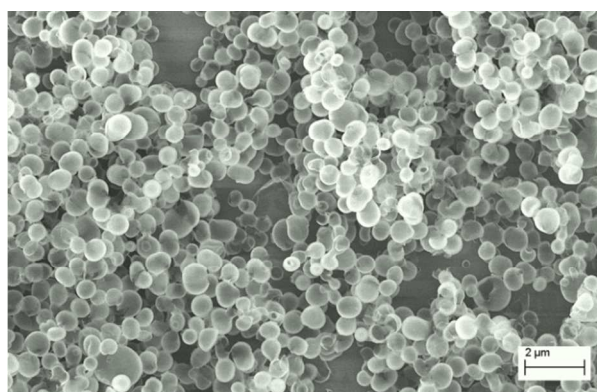


Fig. 6 SEM images of the **1B** nanospheres in DCM–Hexane mixture.

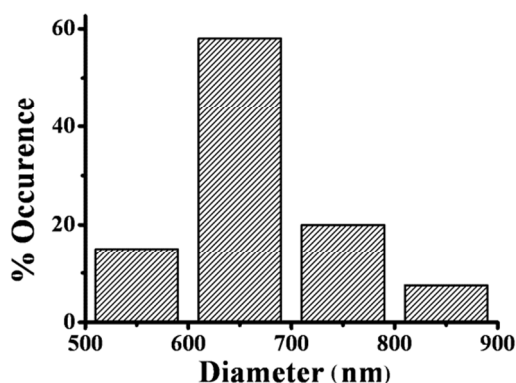


Fig. 7 Particle size distribution histograms of nanospheres of **1B**.

intermolecular interactions exist and three-dimensional networks for those molecules where there is a significant intermolecular interaction. In the present case of study, as the density of DCM is higher than that of water and also due to the presence of significant intermolecular interaction in the complexes **1B**, and **3B**, three-dimensional well organized objects were formed specifically in **1B** and **3B** only. With reference to this, it should be mentioned here, that from X-ray crystal structure analysis it has been observed that intermolecular interactions resulted in the

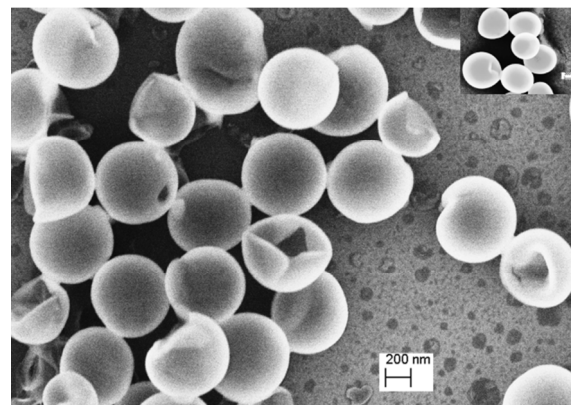


Fig. 8 SEM images of the **3B** in DCM–Hexane mixture; nanospheres are seen.

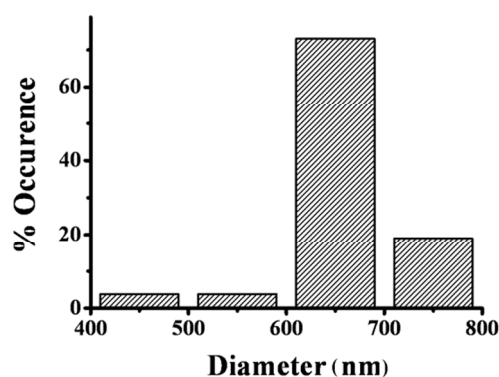


Fig. 9 Particle size distribution histograms of nanospheres of **3B**.

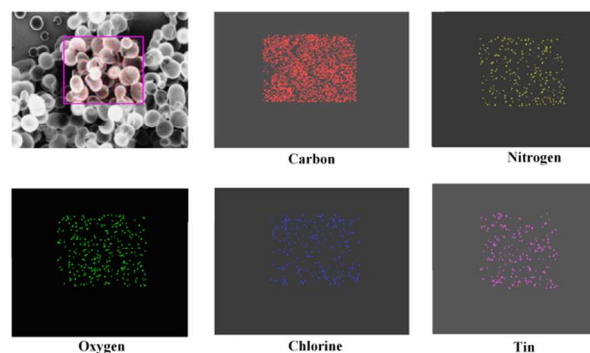
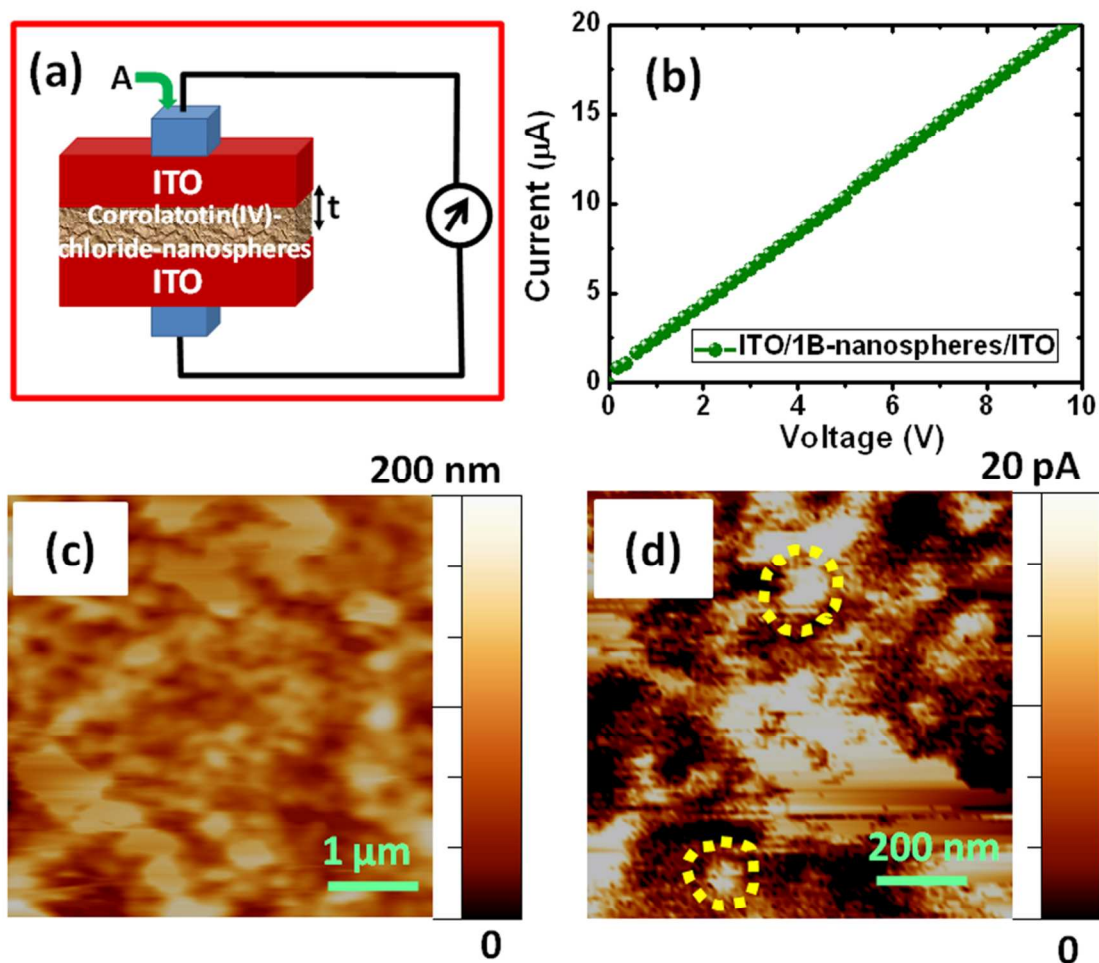


Fig. 10 EDX element map obtained from the surface of the nanospheres of **1B** showing the presence of the entire constituent elements: C, N, O, Sn and Cl.

formation of 1D infinite polymer chains in **1B** and **3B** only but not in the case of **2B**. The justification behind the formation of three-dimensional objects with specific morphology can be understood with the help of solute-solvent interaction during the solvation processes which affects the thermodynamic and kinetic factors for the generation of aggregates.<sup>56-57</sup> EDAX analysis of the individual nanospheres obtained from **1B** molecules clearly confirm their composition and it indicates that spheres are actually composed of **1B** molecules only (Fig. 10).



**Fig. 11** (a) Schematic presentation of the device {Ag/ITO/1B-nanospheres/ITO/Ag}, (b)  $I$ - $V$  characteristics of the device, (c) AFM images showed the 1B-nanospheres, and (d) Current mapping of 1B-nanospheres by conductive atomic force microscopy.

5 All the elements of **1B** are present in those spheres and their weight percentages are also very close to their actual weight percentages in the **1B** molecules. EDAX analysis of the individual nanospheres obtained from **3B** molecules also generates same information like **1B** molecules (Fig. S11†).

#### 10 $I$ - $V$ characteristics and CAFM measurements

A device was fabricated with the following composition: Ag/ITO-coated glass/1B-nanospheres/ITO-coated glass/Ag (see the experimental section and Fig. 11a). Fig. 11b shows  $I$ - $V$  characteristics of the device. From the  $I$ - $V$  characteristics, it appears that the current increases linearly with increasing voltage, indicating an Ohmic characteristic of the device. It also appears that the potential barrier at the interface between the ITO/1B-nanospheres is very low. The resistance of the nanostructured film, generated from 1B-nanospheres, has been obtained from the reciprocal of the slope of the  $I$ - $V$  plot. The observed resistance was found to be  $\sim 4.8 \times 10^7 \Omega$ . From the  $I$ - $V$  plots, it appears that the Ohmic characteristic of the device is maintained up to +10 V.

This observation is a significant improvement from the earlier values as reported by Schwab *et al.*<sup>58</sup> They used the self-assembled nanorods obtained from meso-tetrakis(4-sulfonatophenyl)porphine for the first time and observed that in the dark it acts like an insulator in the voltage range of -0.5 to +0.5 V, with a resistance of  $2.4 \times 10^8 \Omega$ . This resistance value is very close to our observed resistance value. The resistivity ( $\rho$ ) of the nanostructured film was obtained by using the equation<sup>59</sup>:  $\rho = RA/t$ , where  $R$  is the resistance,  $A$  is the effective area of the electrode, and  $t$  is the thickness of the nanostructured film (Fig. 11a). The effective thickness of the nanostructured film was confirmed from the AFM height profile which turned out to be  $\sim 200$  nm (Fig. 11c) and thus, perfectly suits for device application. By making an assumption that the thickness of the nanostructured film is uniform over the ITO surface, the resistivity ( $\rho$ ) of the device was calculated to be  $\sim 2.4 \times 10^8 \Omega \cdot \text{cm}$  and was found to fall in the zone of semi-insulating materials. These semi-insulators have found extensive applications in developing high-electron-mobility transistors. To understand the current conduction pathways in the device and also the local

electrical properties, conductive atomic force microscopy (cAFM) measurements of the **1B**-nanospheres/ITO configuration were performed by using a Pt coated Si tip (radius ~ 30 nm). Stable images were obtained upon continuous scans on different regions of the device and confirm that the molecules are uniformly and strongly bound to the ITO surface. cAFM current maps at 10 V bias show bright spots with 10–20 pA intensity (Fig. 11d) which indicate that nano-spheres are preferentially electron-conducting pathways in the device. It is evident from the CAFM measurements that these active domains are spherical in shape with an average size of ~250 nm in diameter (shown by the yellow circle in Fig. 11d). The semi-insulating behaviour of the nanospheres can be easily understood from the qualitative model described by Schwab *et al.* All the measurements were carried out in dark (i.e., no photo excitation was present during the experiment). We can consider the aggregated Sn(IV) corrole based nanospheres as assemblies/groups of Sn(IV) corrole molecules. The spatially localized HOMOs of the Sn(IV) corrole molecules<sup>60a</sup> are the conduction pathways in the device. As the electron coupling is less in filled HOMOs, therefore, electron transfer occurs mainly through hopping mechanism. Electron transports through filled HOMOs are not at all facile and it requires the access of the higher energy levels as discussed in earlier reports.<sup>58, 60b</sup>

## Conclusions

We have presented here the synthesis of three novel tin(IV)corrole derivatives. Purity and identity of these tin(IV)corroles derivatives have been demonstrated by various spectroscopic techniques and elemental analysis. The <sup>1</sup>H NMR spectra of the tin(IV)corroles derivatives show sharp resonances, which indicate their diamagnetic characteristics. Careful observation of the packing diagrams of **1B** and **3B** reveals assemblies of one dimensional (1D) polymeric chains composed of corrolato-tin(IV)-chloride throughout the crystal lattice. The C–H...Cl hydrogen bonding interaction is the driving force for this kind of supra-molecular 1D chain formation. However in case of **2B**, packing diagram indicate that neighbouring corrolato-tin(IV)-chloride molecules are interconnected by intermolecular C–H...Cl hydrogen bonding interactions to form dimers. In the cases of complexes **1B** and **3B**, well defined and nicely organized three-dimensional hollow nanospheres with diameter of ca. 676 nm (**1B**) and 661 nm (**3B**) were obtained (SEM images on silicon wafers). However in the case of complex **2B**, no such three-dimensional well organized objects were obtained. A device was fabricated with the following compositions: Ag/ITO-coated glass/**1B**-nanospheres/ITO-coated glass/Ag. The resistance of the nanostructured film, generated from **1B**-nanospheres, has been obtained from the the slope of the *I-V* plot. The observed resistance was found to be ~ 4.8×10<sup>7</sup> Ω, which falls in the range of semi-insulating materials. cAFM current maps at 10 V bias showed bright spots with 10–20 pA intensity confirming the fact that nanospheres are preferentially electron-conducting pathways in the device. The spatially localized HOMOs of the Sn(IV) corrole molecules have been speculated to be the conduction pathways in the device. From the obtained resistivity profile, the nanostructured film can be better called as a semi-insulator. These semi-insulating tin(IV) corroles can be useful from the

perspective of the construction of high-electron-mobility transistors (HEMT).

## Experimental section

### Materials

The precursors pyrrole, *p*-chloranil, and 2,4,5-trimethoxybenzaldehyde were purchased from Aldrich, USA. 4-cyano benzaldehyde, 4-bromo benzaldehyde and tin(II) chloride were purchased from Merck, India. Other chemicals were of reagent grade. Hexane and CH<sub>2</sub>Cl<sub>2</sub> were distilled from KOH and CaH<sub>2</sub> respectively. For spectroscopy and electrochemical studies HPLC grade solvents were used. The free base corroles 10-(2,4,5-Trimethoxyphenyl)-5,15-bis(4-cyanophenyl)corrole, **1A**,<sup>51</sup> 5,10,15-Tris(4-cyanophenyl)corrole, **2A**,<sup>52</sup> and 10-(4-Bromophenyl)-5,15-bis(4-cyanophenyl)corrole, **3A**<sup>51</sup> were prepared according to published procedures.

### Characterization

UV–Vis spectral studies were performed on a Perkin–Elmer LAMBDA-750 spectrophotometer. Emission spectral studies were performed on a Perkin Elmer, LS 55 spectrophotometer using optical cell of 1 cm path length. The elemental analyses were carried out with a Perkin–Elmer 240C elemental analyzer. The NMR measurements were carried out using a Bruker AVANCE 400 NMR spectrometer. Chemical shifts are expressed in parts per million (ppm) relative to residual chloroform (δ= 7.26). Electrospray mass spectra were recorded on a Bruker Micro TOF–QII mass spectrometer. SEM images of the nanoparticles were captured by using a field emission gun scanning electron microscope (FEGSEM) system (Zeiss, Germany make, Supra 55). For fabrication of tin(IV) corrole based devices, ITO-coated glass was used as the substrate. The electrical transport property of Ag/ITO-coated glass/**1B**-nanospheres/ITO-coated glass/Ag was measured by studying *I-V* characteristics using a source meter (Keithley, 2410) based measurement setup. All measurements were carried out on several sets of samples to ensure the repeatability and reproducibility. Conducting atomic force microscopy (cAFM) was used to measure the local electric properties of the samples. cAFM was carried out by *ex-situ* atomic force microscopy (AFM) (Asylum Research, MFP3D) in the contact mode with a Pt coated Si cantilever (from NT-MDT) having a radius of curvature of ~35 nm. For each sample, several images were taken from different regions to check the uniformity and to estimate the average conducting area.

### Crystal Structure Determination

Single crystals of 10-(2,4,5-Trimethoxyphenyl)-5,15-bis(4-cyanophenyl)corrolato-tin(IV)-chloride, **1B**, 5,10,15-tris(4-cyanophenyl)corrolato-tin(IV)-chloride, **2B** and 10-(4-bromophenyl)-5,15-bis(4-cyanophenyl)corrolato-tin(IV)-chloride, **3B** were grown by slow diffusion of solutions of the **1B**, **2B** and **3B** in dichloromethane into hexane, followed by slow evaporation under atmospheric conditions. The crystal data of **1B**, **2B** and **3B** were collected on a Bruker Kappa APEX II CCD diffractometer at 293 K. Selected data collection parameters and other crystallographic results are summarized in Table 1. All data were corrected for Lorentz polarization and absorption effects. The program package SHELXTL<sup>61</sup> was used for structure

solution and full matrix least squares refinement on  $F^2$ . Hydrogen atoms were included in the refinement using the riding model. Disordered solvent molecules were taken out using SQUEEZE<sup>62</sup> command in PLATON. CCDC 988125, CCDC 988126, and CCDC 988127 contain the supplementary crystallographic data for **1B**, **2B**, and **3B** respectively. These data can be obtained free of charge via [www.ccdc.cam.ac.uk/data\\_request/cif](http://www.ccdc.cam.ac.uk/data_request/cif).

### Syntheses

#### 10-(2,4,5-Trimethoxyphenyl)-5,15-

#### bis(4-cyanophenyl)corrolato-tin(IV)-chloride, **1B**

**1B** was prepared by slight modifications of the available procedure of corrolato-tin(IV)-chloride synthesis.<sup>47</sup> 100 mg (0.15 mmol) of the free base corrole, **1A** was dissolved in 20 mL of DMF. Then 285 mg (1.50 mmol) of tin(II) chloride was added to the reaction vessel under reflux condition and the stirring was continued till 1 h. Formation of the product was confirmed by TLC examination. The solvent was removed completely by rotary evaporation. The crude product was then purified by column chromatography using silica gel (100-200 mesh) with dichloromethane as eluent. After recrystallization from dichloromethane and hexane, 81 mg (100  $\mu$ mol) of pure crystalline compound was collected (66%). Anal. Calcd (found) for  $C_{42}H_{27}ClN_6O_3Sn$  (**1B**): C, 61.68 (61.52); H, 3.33 (3.49); N, 10.28 (10.13).  $\lambda_{max}/nm$  ( $\epsilon/M^{-1}cm^{-1}$ ) in dichloromethane: 423 (176330), 532 (5477), 572 (9850), 605 (24910) (Fig. S1<sup>†</sup>). <sup>1</sup>H NMR (400 MHz,  $CDCl_3$ )  $\delta$  9.28 – 9.25 (m, 2H), 9.09 – 9.03 (m, 2H), 8.87 – 8.85 (m, 2H), 8.81 – 8.79 (m, 2H), 8.12 (broad s, 8H), 7.78 (s, 1H), 6.94 (s, 1H), 4.19 (s, 3H), 4.01 (s, 3H), 3.37 (s, 3H). **1B** displayed strong fluorescence at 618.5 nm and 673 nm in dichloromethane (Fig. 1). The electrospray mass spectrum of **1B** in acetonitrile showed peaks centered at  $m/z = 818.07$  corresponding to [**1B**]<sup>+</sup> (818.08 calcd for  $C_{42}H_{27}ClN_6O_3Sn$ ).

#### 5,10,15-tris(4-cyanophenyl)-corrolato-tin(IV)-chloride, **2B**

**2B** was synthesized by a procedure similar to **1B**, starting with 100 mg (0.166 mmol) of the free base corrole, **2A** and 315.5 mg (1.66 mmol) of tin(II) chloride. The crude product was purified by column chromatography using silica gel (100-200 mesh) with 20% MeCN and 80% dichloromethane as eluent. After purification, the compound was kept for recrystallization to afford crystals of **2B** (81 mg, 110  $\mu$ mol, 67%). Anal. Calcd (found) for  $C_{40}H_{20}ClN_7Sn$  (**2B**): C, 63.82 (63.69); H, 2.68 (2.78); N, 13.02 (12.91).  $\lambda_{max}/nm$  ( $\epsilon/M^{-1}cm^{-1}$ ) in dichloromethane: 424 (210000), 532 (10556), 569 (13037), 604 (27927) (Fig. S1<sup>†</sup>). <sup>1</sup>H NMR (400 MHz,  $CDCl_3$ )  $\delta$  9.36 – 9.31 (m, 2H), 9.16 – 9.12 (m, 2H), 8.88 – 8.84 (m, 4H), 8.57 (d,  $J = 7.5$  Hz, 2H), 8.35 – 7.84 (m, 10H). **2B** displayed strong fluorescence at 619 nm and 672.5 nm in dichloromethane (Fig. 1). The electrospray mass spectrum of 5,10,15-tris(4-cyanophenyl)-corrolato-tin(IV)-chloride, **2B** in acetonitrile showed peaks centered at  $m/z = 753.034$  corresponding to [**2B**]<sup>+</sup> (753.049 calcd for  $C_{40}H_{20}ClN_7Sn$ ).

#### 10-(4-Bromophenyl)-5,15-bis(4-cyanophenyl)-corrolato-tin(IV)-chloride, **3B**

**3B** was synthesized by a procedure similar to **1B**, starting with 100 mg (0.153 mmol) of the free base corrole, **3A** and 290.1 mg (1.53 mmol) of tin(II) chloride. The crude product was then purified by column chromatography using silica gel (100-200

mesh) with 20% MeCN and 80% dichloromethane as eluent. After purification, the compound was kept for recrystallization to afford crystals of **3B** (85 mg, 110  $\mu$ mol, 69%). Anal. Calcd (found) for  $C_{39}H_{20}BrClN_6Sn$  (**3B**): C, 58.07 (58.52); H, 2.50 (2.60); N, 10.42 (10.79).  $\lambda_{max}/nm$  ( $\epsilon/M^{-1}cm^{-1}$ ) in dichloromethane: 423 (160700), 529 (6680), 570 (7251), 606 (18995) (Fig. S1<sup>†</sup>). <sup>1</sup>H NMR (400 MHz,  $CDCl_3$ )  $\delta$  9.33 – 9.29 (m, 2H), 9.14 – 9.08 (m, 2H), 8.95 – 8.90 (m, 2H), 8.86 – 8.81 (m, 2H), 8.30 – 7.82 (m, 12H). <sup>13</sup>C NMR (101 MHz,  $CDCl_3$ )  $\delta$  111.0, 112.1, 116.4, 118.5, 119.1, 122.9, 126.6, 127.3, 129.2, 130.9, 131.0, 131.7, 135.2, 135.4, 136.2, 138.4, 139.6, 140.2, 143.7, 145.0 (Fig. S2<sup>†</sup>). **3B** displayed strong fluorescence at 618.8 nm and 671 nm in dichloromethane (Fig. 1). The electrospray mass spectrum of 10-(4-bromophenyl)-5,15-bis(4-cyanophenyl)-corrolato-tin(IV)-chloride, **3B** in acetonitrile showed peaks centered at  $m/z = 771.001$  corresponding to [**3B**-Cl]<sup>+</sup> (770.995 calcd for  $C_{39}H_{20}BrN_6Sn$ ).

### Acknowledgements

Financial support received from the Department of Atomic Energy, (India) is gratefully acknowledged. S.K. thanks DST-New Delhi for partial funding. Authors thankfully acknowledge NISER, Bhubaneswar and IOP, Bhubaneswar for providing infrastructure and instrumental supports.

### Notes and references

<sup>a</sup>School of Chemical Sciences, National Institute of Science Education and Research (NISER), Bhubaneswar – 751005, India. E-mail: [sanjib@niser.ac.in](mailto:sanjib@niser.ac.in)  
<sup>b</sup>Institute of Physics, Sachivalaya Marg, Bhubaneswar – 751005, India. E-mail: [tson@iop.res.in](mailto:tson@iop.res.in)

<sup>†</sup> Electronic Supplementary Information (ESI) available: Single-crystal X-ray structure analysis of **1B**, **2B** and **3B**. ESI- MS spectrum of **1B**, **2B** and **3B**. <sup>1</sup>H NMR spectrum of **1B**, **2B** and **3B**. <sup>13</sup>C NMR spectra of **3B**. EDX elemental analysis of **3B**. CCDC 988125, CCDC 988126, and CCDC 988127 contain the supplementary crystallographic data for **1B**, **2B**, and **3B** respectively. These data can be obtained free of charge via [www.ccdc.cam.ac.uk/data\\_request/cif](http://www.ccdc.cam.ac.uk/data_request/cif). See DOI: 10.1039/b000000x/

- G. McDermott, S. M. Prince, A. A. Freer, A. M. Hawthornthwaite-Lawless, M. Z. Papiz, R. J. Cogdell and N. W. Isaacs, *Nature (London)*, 1995, **374**, 517-521.
- S. Bahatyrova, R. N. Frese, C. A. Siebert, J. D. Olsen, K. O. van der Werf, R. van Grondelle, R. A. Niederman, P. A. Bullough, C. Otto and C. N. Hunter, *Nature (London, U. K.)*, 2004, **430**, 1058-1062.
- A. K. Burrell, D. L. Officer, P. G. Plieger and D. C. W. Reid, *Chem. Rev. (Washington, D. C.)*, 2001, **101**, 2751-2796.
- D. Kim and A. Osuka, *Acc. Chem. Res.*, 2004, **37**, 735-745.
- T. S. Balaban, A. D. Bhise, M. Fischer, M. Linke-Schaetzl, C. Roussel and N. Vanthuyne, *Angew. Chem., Int. Ed.*, 2003, **42**, 2140-2144.
- M. Linke-Schaetzl, A. D. Bhise, H. Gliemann, T. Koch, T. Schimmel and T. S. Balaban, *Thin Solid Films*, 2004, **451-452**, 16-21.
- T. S. Balaban, M. Linke-Schaetzl, A. D. Bhise, N. Vanthuyne, C. Roussel, C. E. Anson, G. Buth, A. Eichhoefer, K. Foster, G. Garab, H. Gliemann, R. Goddard, T. Javorfi, A. K. Powell, H. Roesner and T. Schimmel, *Chem. - Eur. J.*, 2005, **11**, 2267-2275.
- J. Otsuki, K. Iwasaki, Y. Nakano, M. Itou, Y. Araki and O. Ito, *Chem. - Eur. J.*, 2004, **10**, 3461-3466.

- 9 J. M. Ribo, J. Crusats, F. Sagues, J. Claret and R. Rubires, *Science (Washington, DC, U. S.)*, 2001, **292**, 2063-2066.
- 10 Z. Wang, C. J. Medforth and J. A. Shelnutt, *J. Am. Chem. Soc.*, 2004, **126**, 15954-15955.
- 5 11 R. Takahashi and Y. Kobuke, *J. Am. Chem. Soc.*, 2003, **125**, 2372-2373.
- 12 P. G. Schouten, J. M. Warman, M. P. De Haas, M. A. Fox and H. L. Pan, *Nature (London)*, 1991, **353**, 736-737.
- 13 S. Patwardhan, S. Sengupta, L. D. A. Siebbeles, F. Wuerthner and F. C. Grozema, *J. Am. Chem. Soc.*, 2012, **134**, 16147-16150.
- 10 14 A. P. H. J. Schenning and E. W. Meijer, *Chem. Commun. (Cambridge, U. K.)*, 2005, 3245-3258.
- 15 S. Sengupta and F. Wuerthner, *Acc. Chem. Res.*, 2013, **46**, 2498-2512.
- 15 16 (a) K. M. Kadish, K. M. Smith and R. Guilard (eds.), *The Porphyrin Handbook*, Academic Press, New York, 1959-2003, vol. 1-20; (b) S. Cai, S. Licoecia and F. A. Walker, *Inorg. Chem.*, 2001, **40**, 5795-5798; (c) B. Ramdhanie, L. N. Zakharov, A. L. Rheingold and D. P. Goldberg, *Inorg. Chem.*, 2002, **41**, 4105-4107; (d) K. M. Kadish, L. Fremond, Z. Ou, J. Shao, C. Shi, F. C. Anson, F. Burdet, C. P. Gros, J.-M. Barbe and R. Guilard, *J. Am. Chem. Soc.*, 2005, **127**, 5625-5631; (e) J. P. Collman and R. A. Decreau, *Org. Lett.*, 2005, **7**, 975-978; (f) N. Y. Edwards, R. A. Eikey, M. I. Loring and M. M. Abu-Omar, *Inorg. Chem.*, 2005, **44**, 3700-3708; (g) D. T. Gryko, J. P. Fox and D. P. Goldberg, *J. Porphyrins Phthalocyanines*, 2004, **8**, 1091-1105; (h) E. Van Caemelbecke, S. Will, M. Autret, V. A. Adamian, J. Lex, J.-P. Gisselbrecht, M. Gross, E. Vogel and K. M. Kadish, *Inorg. Chem.*, 1996, **35**, 184-192; (i) A. Mahammed, H. B. Gray, A. E. Meier-Callahan and Z. Gross, *J. Am. Chem. Soc.*, 2003, **125**, 1162-1163; (j) M. Hoshino, K. Ozawa, H. Seki and P. C. Ford, *J. Am. Chem. Soc.*, 1993, **115**, 9568-9575; (k) M. Hoshino, M. Maeda, R. Konishi, H. Seki and P. C. Ford, *J. Am. Chem. Soc.*, 1996, **118**, 5702-5707; (l) L. E. Laverman, M. Hoshino and P. C. Ford, *J. Am. Chem. Soc.*, 1997, **119**, 12663-12664; (m) I. M. Lorkovic and P. C. Ford, *Inorg. Chem.*, 1999, **38**, 1467-1473; (n) D. N. Harischandra, R. Zhang and M. Newcomb, *J. Am. Chem. Soc.*, 2005, **127**, 13776-13777; (o) E. Vogel, S. Will, A. S. Tilling, L. Neumann, J. Lex, E. Bill, A. X. Trautwein and K. Wieghardt, *Angew. Chem., Int. Ed.*, 1994, **33**, 731-735; (p) R. Guilard, C. P. Gros, F. Bolze, F. Jerome, Z. Ou, J. Shao, J. Fischer, R. Weiss and K. M. Kadish, *Inorg. Chem.*, 2001, **40**, 4845-4855; (q) K. M. Kadish, Z. Ou, V. A. Adamian, R. Guilard, C. P. Gros, C. Erben, S. Will and E. Vogel, *Inorg. Chem.*, 2000, **39**, 5675-5682; (r) C. P. Gros, J.-M. Barbe, E. Espinosa and R. Guilard, *Angew. Chem., Int. Ed.*, 2006, **45**, 5642-5645; (s) X. Liang, J. Mack, L.-M. Zheng, Z. Shen and N. Kobayashi, *Inorg. Chem.*, 2014, **53**, 2797-2802; (t) B. Brizet, N. Desbois, A. Bonnot, A. Langlois, A. Dubois, J.-M. Barbe, C. P. Gros, C. Goze, F. Denat and P. D. Harvey, *Inorg. Chem.*, 2014, **53**, 3392-3403; (u) R. Padilla, H. L. Buckley, A. L. Ward and J. Arnold, *Chem. Commun.*, 2014, **50**, 2922-2924; (v) C. P. Gros, F. Brisach, A. Meristoudi, E. Espinosa, R. Guilard and P. D. Harvey, *Inorg. Chem.*, 2007, **46**, 125-135; (w) K. M. Kadish, J. Shen, L. Fremond, P. Chen, M. El Ojaimi, M. Chkounda, C. P. Gros, J.-M. Barbe, K. Ohkubo, S. Fukuzumi and R. Guilard, *Inorg. Chem.*, 2008, **47**, 6726-6737.
- 17 J. Bendix, I. J. Dmochowski, H. B. Gray, A. Mahammed, L. Simkhovich and Z. Gross, *Angew. Chem., Int. Ed.*, 2000, **39**, 4048-4051.
- 60 18 S. Cho, J. M. Lim, S. Hiroto, P. Kim, H. Shinokubo, A. Osuka and D. Kim, *J. Am. Chem. Soc.*, 2009, **131**, 6412-6420.
- 19 F. D'Souza, R. Chitta, K. Ohkubo, M. Tasior, N. K. Subbaiyan, M. E. Zandler, M. K. Rogacki, D. T. Gryko and S. Fukuzumi, *J. Am. Chem. Soc.*, 2008, **130**, 14263-14272.
- 65 20 L. Flamigni and D. T. Gryko, *Chem. Soc. Rev.*, 2009, **38**, 1635-1646.
- 21 Y. Gao, J. Liu, W. Jiang, M. Xia, W. Zhang, M. Li, B. Akermark and L. Sun, *J. Porphyrins Phthalocyanines*, 2007, **11**, 463-469.
- 22 S. Nardis, F. Mandoj, R. Paolesse, F. R. Fronczek, K. M. Smith, L. Prodi, M. Montalti and G. Battistini, *Eur. J. Inorg. Chem.*, 2007, 2345-2352.
- 70 23 T. H. Ngo, F. Nastasi, F. Puntoriero, S. Campagna, W. Dehaen and W. Maes, *Eur. J. Org. Chem.*, 2012, 5605-5617.
- 24 J. H. Palmer, T. Brock-Nannestad, A. Mahammed, A. C. Durrell, D. Vander Velde, S. Virgil, Z. Gross and H. B. Gray, *Angew. Chem., Int. Ed.*, 2011, **50**, 9433-9436.
- 75 25 R. Paolesse, F. Sagone, A. Macagnano, T. Boschi, L. Prodi, M. Montalti, N. Zaccheroni, F. Bolletta and K. M. Smith, *J. Porphyrins Phthalocyanines*, 1999, **3**, 364-370.
- 80 26 K. Peuntinger, T. Lazarides, D. Dafnomili, G. Charalambidis, G. Landrou, A. Kahnt, R. P. Sabatini, D. W. McCamant, D. T. Gryko, A. G. Coutsolelos and D. M. Guldi, *J. Phys. Chem. C*, 2013, **117**, 1647-1655.
- 27 E. Steene, T. Wondimagegn and A. Ghosh, *J. Phys. Chem. B*, 2001, **105**, 11406-11413.
- 85 28 E. Rabinovich, I. Goldberg and Z. Gross, *Chem. - Eur. J.*, 2011, **17**, 12294-12301.
- 29 E. Stavitski, A. Berg, T. Ganguly, A. Mahammed, Z. Gross and H. Levanon, *J. Am. Chem. Soc.*, 2004, **126**, 6886-6890.
- 90 30 M. Tasior, D. T. Gryko, M. Cembor, J. S. Jaworski, B. Ventura and L. Flamigni, *New J. Chem.*, 2007, **31**, 247-259.
- 31 M. Tasior, D. T. Gryko, J. Shen, K. M. Kadish, T. Becherer, H. Langhals, B. Ventura and L. Flamigni, *J. Phys. Chem. C*, 2008, **112**, 19699-19709.
- 95 32 B. Ventura, A. Degli Esposti, B. Koszarna, D. T. Gryko and L. Flamigni, *New J. Chem.*, 2005, **29**, 1559-1566.
- 33 L. Wagnert, R. Rubin, A. Berg, A. Mahammed, Z. Gross and H. Levanon, *J. Phys. Chem. B*, 2010, **114**, 14303-14308.
- 34 J. L. Sessler and S. J. Weghorn, in *Expanded, Contracted & Isomeric Porphyrin*, ed. J. E. Baldwin, Tetrahedron Organic Chemistry Series, Pergamon, New York, 1997, vol. 18, pp. 11-120.
- 100 35 I. Aviv and Z. Gross, *Chem. Commun. (Cambridge, U. K.)*, 2007, 1987-1999.
- 36 I. Aviv-Harel and Z. Gross, *Chem. - Eur. J.*, 2009, **15**, 8382-8394.
- 105 37 I. Aviv-Harel and Z. Gross, *Coord. Chem. Rev.*, 2011, **255**, 717-736.
- 38 T. Ding, E. A. Aleman, D. A. Modarelli and C. J. Ziegler, *J. Phys. Chem. A*, 2005, **109**, 7411-7417.
- 39 B. Koszarna and D. T. Gryko, *Chem. Commun. (Cambridge, U. K.)*, 2007, 2994-2996.
- 110 40 C. I. M. Santos, E. Oliveira, J. F. B. Barata, M. A. F. Faustino, J. A. S. Cavaleiro, M. G. P. M. S. Neves and C. Lodeiro, *J. Mater. Chem.*, 2012, **22**, 13811-13819.
- 41 D. Maeda, H. Shimakoshi, M. Abe and Y. Hisaeda, *Inorg. Chem.*, 2009, **48**, 9853-9860.
- 115 42 J. C. Patterson, I. M. Lorkovic and P. C. Ford, *Inorg. Chem.*, 2003, **42**, 4902-4908.
- 43 G. Pomarico, F. R. Fronczek, S. Nardis, K. M. Smith and R. Paolesse, *J. Porphyrins Phthalocyanines*, 2011, **15**, 1085-1092.
- 120 44 G. Pomarico, S. Nardis, M. Stefanelli, D. O. Cicero, M. G. H. Vicente, Y. Fang, P. Chen, K. M. Kadish and R. Paolesse, *Inorg. Chem.*, 2013, **52**, 8834-8844.
- 45 B. O. Fernandez and P. C. Ford, *J. Am. Chem. Soc.*, 2003, **125**, 10510-10511.
- 125 46 (a) K. Chandrasekaran and D. G. Whitten, *J. Am. Chem. Soc.*, 1980, **102**, 5119-5120; (b) D. M. Collins, W. R. Scheidt and J. L. Hoard, *J. Amer. Chem. Soc.*, 1972, **94**, 6689-6696; (c) K. E. Martin, Z. Wang, T. Busani, R. M. Garcia, Z. Chen, Y. Jiang, Y. Song, J. L. Jacobsen, T. T. Vu, N. E. Schore, B. S. Swartzentruber, C. J. Medforth and J. A. Shelnutt, *J. Am. Chem. Soc.*, 2010, **132**, 8194-8201; (d) J. Rodriguez, C. Kirmaier and D. Holten, *J. Am. Chem. Soc.*, 1989, **111**, 6500-6506; (e) Z. Wang, Z. Li, C. J.

- Medforth and J. A. Shelnut, *J. Am. Chem. Soc.*, 2007, **129**, 2440-2441; (f) T. Lang, A. Guenet, E. Graf, N. Kyritsakas and M. W. Hosseini, *Chem. Commun. (Cambridge, U. K.)*, 2010, **46**, 3508-3510; (g) Y. Tian, K. E. Martin, J. Y. T. Shelnut, L. Evans, T. Busani, J. E. Miller, C. J. Medforth and J. A. Shelnut, *Chem. Commun. (Cambridge, U. K.)*, 2011, **47**, 6069-6071; (h) A. Guenet, E. Graf, N. Kyritsakas and M. W. Hosseini, *Inorg. Chem.*, 2010, **49**, 1872-1883; (i) T. Lazarides, S. Kuhri, G. Charalambidis, M. K. Panda, D. M. Guldi and A. G. Coutsolelos, *Inorg. Chem.*, 2012, **51**, 4193-4204; (j) K. T. Oppelt, E. Woess, M. Stiftinger, W. Schoefberger, W. Buchberger and G. Knoer, *Inorg. Chem.*, 2013, **52**, 11910-11922; (k) A. M. Shultz, O. K. Farha, D. Adhikari, A. A. Sarjeant, J. T. Hupp and S. T. Nguyen, *Inorg. Chem.*, 2011, **50**, 3174-3176.
- 47 (a) Y. S. Balazs, I. Saltsman, A. Mahammed, E. Tkachenko, G. Golubkov, J. Levine and Z. Gross, *Magn. Reson. Chem.*, 2004, **42**, 624-635; (b) G. Pomarico, S. Nardis, R. Paolesse, O. C. Ongayi, B. H. Courtney, F. R. Fronczek and M. G. H. Vicente, *J. Org. Chem.*, 2011, **76**, 3765-3773; (c) J. Poulin, C. Stern, R. Guillard and P. D. Harvey, *Photochem. Photobiol.*, 2006, **82**, 171-176; (d) V. Rozenshtein, L. Wagnert, A. Berg, E. Stavitski, T. Berthold, G. Kothe, I. Saltsman, Z. Gross and H. Levanon, *J. Phys. Chem. A*, 2008, **112**, 5338-5343; (e) I. Saltsman, A. Mahammed, I. Goldberg, E. Tkachenko, M. Botoshansky and Z. Gross, *J. Am. Chem. Soc.*, 2002, **124**, 7411-7420; (f) L. Simkhovich, A. Mahammed, I. Goldberg and Z. Gross, *Chem. - Eur. J.*, 2001, **7**, 1041-1055; (g) O. G. Tsay, B.-K. Kim, T. L. Luu, J. Kwak and D. G. Churchill, *Inorg. Chem.*, 2013, **52**, 1991-1999; (h) L. Wagnert, A. Berg, E. Stavitski, T. Berthold, G. Kothe, I. Goldberg, A. Mahammed, L. Simkhovich, Z. Gross and H. Levanon, *Appl. Magn. Reson.*, 2006, **30**, 591-604; (i) D. Walker, S. Chappel, A. Mahammed, B. S. Brunschwig, J. R. Winkler, H. B. Gray, A. Zaban and Z. Gross, *J. Porphyrins Phthalocyanines*, 2006, **10**, 1259-1262; (j) K. M. Kadish, S. Will, V. A. Adamian, B. Walther, C. Erben, Z. Ou, N. Guo and E. Vogel, *Inorg. Chem.*, 1998, **37**, 4573-4577.
- 48 (a) F. Dini, E. Martinelli, G. Pomarico, R. Paolesse, D. Monti, D. Filippini, A. D'Amico, I. Lundstroem and C. Di Natale, *Nanotechnology*, 2009, **20**, 055502/055501-055502/055508; (b) G. Kwag, E. Park and S. Kim, *Bull. Korean Chem. Soc.*, 2004, **25**, 298-300; (c) R. Patra, H. M. Titi and I. Goldberg, *Cryst. Growth Des.*, 2013, **13**, 1342-1349; (d) J. Roales, J. M. Pedrosa, P. Castillero, M. Cano, T. H. Richardson, A. Barranco and A. R. Gonzalez-Elipe, *ACS Appl. Mater. Interfaces*, 2012, **4**, 5147-5154.
- 49 D. S. Bale and C. Szeles, *Phys. Rev. B: Condens. Matter Mater. Phys.*, 2008, **77**, 035205/035201-035205/035216.
- 50 X. Yu, C. Li, Z. N. Low, J. Lin, T. J. Anderson, H. T. Wang, F. Ren, Y. L. Wang, C. Y. Chang, S. J. Pearton, C. H. Hsu, A. Osinsky, A. Dabiran, P. Chow, C. Balaban and J. Painter, *Sens. Actuators, B*, 2008, **135**, 188-194.
- 51 W. Sinha, N. Deibel, H. Agarwala, A. Garai, D. Schweinfurth, C. S. Purohit, G. K. Lahiri, B. Sarkar and S. Kar, *Inorg. Chem.*, 2014, **53**, 1417-1429.
- 52 B. Koszarna and D. T. Gryko, *J. Org. Chem.*, 2006, **71**, 3707-3717.
- 53 Y. Ohgo, S. Neya, T. Ikeue, M. Takahashi, M. Takeda, N. Funasaki and M. Nakamura, *Inorg. Chem.*, 2002, **41**, 4627-4629.
- 54 (a) A. Nangia, *CrystEngComm*, 2002, **4**, 93-101; (b) C. B. Aakeroy, T. A. Evans, K. R. Seddon and I. Palinko, *New J. Chem.*, 1999, **23**, 145-152; (c) V. Balamurugan, W. Jacob, J. Mukherjee and R. Mukherjee, *CrystEngComm*, 2004, **6**, 396-400; (d) V. Balamurugan, M. S. Hundal and R. Mukherjee, *Chem. - Eur. J.*, 2004, **10**, 1683-1690.
- 55 M. Srinivasarao, D. Collings, A. Philips and S. Patel, *Science (Washington, DC, U. S.)*, 2001, **292**, 79-82.
- 56 S. J. Lee, J. T. Hupp and S. T. Nguyen, *J. Am. Chem. Soc.*, 2008, **130**, 9632-9633.
- 57 (a) Y. Gao, X. Zhang, C. Ma, X. Li and J. Jiang, *J. Am. Chem. Soc.*, 2008, **130**, 17044-17052; (b) W. Sinha, N. Deibel, A. Garai, D. Schweinfurth, S. Anwar, C. S. Purohit, B. Sarkar and S. Kar, *Dyes and Pigments*, 2014, **107**, 29-37.
- 58 A. D. Schwab, D. E. Smith, B. Bond-Watts, D. E. Johnston, J. Hone, A. T. Johnson, J. C. De Paula and W. F. Smith, *Nano Lett.*, 2004, **4**, 1261-1265.
- 59 F.-C. Hsu, V. N. Prigodin and A. J. Epstein, *Phys. Rev. B: Condens. Matter Mater. Phys.*, 2006, **74**, 235219/235211-235219/235212.
- 75 60 (a) B. A. Friesen, B. Wiggins, J. L. McHale, U. Mazur and K. W. Hipps, *J. Am. Chem. Soc.*, 2010, **132**, 8554-8556; (b) B. A. Friesen, B. Wiggins, J. L. McHale, U. Mazur and K. W. Hipps, *J. Am. Chem. Soc.*, 2010, **132**, 8554-8556.
- 80 61 G. M. Sheldrick, *Acta Crystallogr., Sect. A: Found. Crystallogr.*, 2008, **64**, 112-122.
- 62 P. Van der Sluis and A. L. Spek, *Acta Crystallogr., Sect. A: Found. Crystallogr.*, 1990, **A46**, 194-201.